Bioorganic & Medicinal Chemistry Letters 21 (2011) 417–422

Contents lists available at ScienceDirect

Bioorganic & Medicinal Chemistry Letters

journal homepage: www.elsevier.com/locate/bmcl

A novel series of IKKβ inhibitors part I: Initial SAR studies of a HTS hit

Timothy D. Cushing [a,*], Vijay Baichwal [b], Karen Berry [d], Roland Billedeau [e], Viola Bordunov [e], Chris Broka [e], Mario Cardozo [c], Peng Cheng [a], David Clark [a], Stacie Dalrymple [f], Michael DeGraffenreid [a], Adrian Gill [e], Xiaolin Hao [a], Ronald C. Hawley [e], Xiao He [a], Juan C. Jaen [a], Sharada S. Labadie [e], Marc Labelle [a], Csaba Lehel [b], Pu-Ping Lu [a], Joel McIntosh [e], Shichang Miao [d], Camran Parast [b], Youngsook Shin [a], Eric B. Sjogren [e], Marie-Louise Smith [a], Francisco X. Talamas [e], George Tonn [d], Keith M. Walker [e], Nigel P. C. Walker [c], Holger Wesche [b], Chris Whitehead [e], Matt Wright [d], Michelle F. Browner [g]

[a] Medicinal Chemistry, Amgen Inc., 1120 Veterans Blvd., South San Francisco, CA 94080, USA
[b] Inflammation Biology, Amgen Inc., 1120 Veterans Blvd., South San Francisco, CA 94080, USA
[c] Molecular Structure, Amgen Inc., 1120 Veterans Blvd., South San Francisco, CA 94080, USA
[d] Pharmacokinetics and Drug Metabolism, Amgen Inc., 1120 Veterans Blvd., South San Francisco, CA 94080, USA
[e] Chemistry, Roche Palo Alto, Hillview Ave., Palo Alto, CA 94304, USA
[f] Biology, Roche Palo Alto, Hillview Ave., Palo Alto, CA 94304, USA
[g] Discovery Technologies, Roche Palo Alto, Hillview Ave., Palo Alto, CA 94304, USA

ARTICLE INFO

Article history:
Received 8 September 2010
Revised 22 October 2010
Accepted 25 October 2010
Available online 29 October 2010

Keywords:
IKKβ
IKKα
Semithiocarbazones
Semicarbazones

ABSTRACT

A novel series of (*E*)-1-((2-(1-methyl-1*H*-imidazol-5-yl) quinolin-4-yl) methylene) thiosemicarbazides was discovered as potent inhibitors of IKKβ. In this Letter we document our early efforts at optimization of the quinoline core, the imidazole and the semithiocarbazone moiety. Most potency gains came from substitution around the 6- and 7-positions of the quinoline ring. Replacement of the semithiocarbazone with a semicarbazone decreased potency but led to some measurable exposure.

The highly homologous IKKβ and IKKα are members of a small class of protein kinases known as IκB Kinases (IKKs).[1] They have a distinct role in the regulation of both adaptive and innate immunity and are critical for most aspects of host defense.[2] IKKβ and IKKα activity are required for the activation of the transcription factor Nuclear Factor kappa B (NF-κB). NF-κB controls much of the innate immune system and is instrumental in the induction of genes leading to a pro-inflammatory response. In the classical NF-κB pathway, IKKβ and IKKα form a heteromeric dimer, which after activation (cytokine signaling) leads to a larger complex with the ancillary proteins TRAF2/5, RIP1, TRADD, and IKKγ. Phosphorylation of two key serines in part of the IκB/NF-κB complex causes the protein to be polyubiquitinated, and degraded. This allows the unbound NF-κB dimers to translocate to the nucleus, initiate gene transcription ultimately leading to pro-inflammatory cytokine production. In the alternative NF-κB pathway, involved in adaptive immunity, activation of certain tumor necrosis factor receptor (TNFR) family members (e.g., BAFF receptor) leads to the activation of the kinase NIK, which recruits IKKα and binds to p100, the NF-κB precursor. NIK phosphorylates IKKα, and IKKα in turn phosphorylates p100 leading to its polyubiquitination, partial degradation and activation. NF-κB then translocates to the nucleus initiating the transcriptional machinery. IKKβ and IKKα clearly play a central role in activation of NF-κB with IKKβ proving indispensable for the activation of the classical NF-κB pathway.[3]

Aberrant activation of the NF-κB pathway has been implicated in inflammation, autoimmune diseases and cancer.[4] Thus, drugs[5] targeting these kinases are very promising candidates for the treatment of many diseases.[6] While the role of IKKβ is limited to the activation of NF-κB, IKKα is thought to be involved in other processes, including skin development, and the termination of an inflammatory response,[7] hence selective inhibitors of IKKβ are highly desirable.

In this Letter, we describe our preliminary efforts to understand the SAR, pharmacokinetics and pharmacology of a unique class of molecules that inhibit IKKβ. Compound **1** (Fig. 1) was identified through high throughput screening (HTS). It is ATP competitive,

* Corresponding author.
E-mail address: tcushing@amgen.com (T.D. Cushing).

0960-894X/$ - see front matter © 2010 Elsevier Ltd. All rights reserved.
doi:10.1016/j.bmcl.2010.10.126

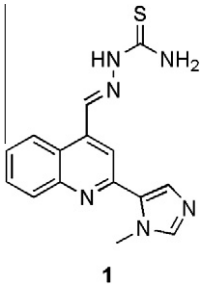

1

Figure 1. Lead compound **1**, obtained by high throughput screening.

reversible, potent, and selective over IKKα, (IC_{50} IKKβ = 0.25 μM, IC_{50} IKKα = 9.19 μM). It is also selective (>30 μM) over several other kinases: JAK3, NIK, IRAK, PKA, PKC, c-Src, Abl, and RIP. Although **1** represents a promising lead with respect to its inhibition of IKKβ and its selectivity profile, it demonstrated poor aqueous solubility (3.1 μg/mL, PBS buffer).

Our initial SAR efforts focused on the identification of the pharmacophore, optimization of the potency and improvement of the physico-chemical properties. Compound **1** could be subdivided into three main regions; a quinoline core, a semithiocarbazone and a methylimidazole ring. Analogs were prepared via a variety of synthetic routes.[8] The main route employed a Pfitzinger condensation between an isatin (**A)** and an imidazole ketone, such as **F**. The resulting carboxylic acid was manipulated by standard methods to provide an aldehyde (**D**), which was then condensed with various nucleophiles to provide a generalized analog **E** (Scheme 1).

Most of the analogs in Table 1 were prepared by the method of Scheme 1. To explore the SAR around positions 2 and 4 of the quinoline core, Scheme 2 was generally followed. The analogs of Table 2 were prepared by routes 2D, and 2E and Scheme 1. Many of the analogs in Table 3 were prepared by employing alternative heterocyclic methyl ketones for intermediate **F** (Scheme 1). Other analogs in Table 3 were prepared by the chemistry outlined in Scheme 2B and C. Routes 2A and 2C and variants thereof were used in the synthesis of analogs found in Table 4. The majority of the compounds in Table 5 followed Scheme 1. Reduction (hydrogenation) of the R_1-group prior to the final nucleophilic alkylation provided analogs such as **69** and **70** (step g, Scheme 1).

There were several assays used to develop the SAR in this program. Our primary biochemical assay was a chemiluminescent ELISA assay against IKKβ and IKKα.[9]

Our main cellular assays were an NF-κB activation assay[10] (gel-shift assay induced with TNF) and a human whole blood (HWB) assay induced by lipopolysaccharide (LPS).[11]

Table 1
SAR of the semithiocarbazone

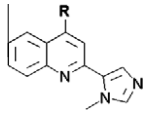

Compds	R	IKKβ IC_{50} (μM)
1	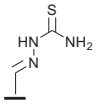	0.25
2	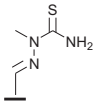	0.12
3	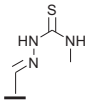	1.7
4	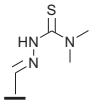	>30
5	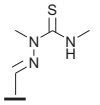	>30
6	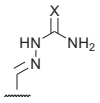	X = O: 1.1
7		X = NH: 17
8	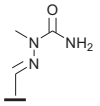	7.8
9	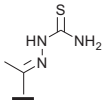	>30

One initial goal of our SAR efforts was to understand the role of the semithiocarbazone, which we believed could prove a liability. A small series of changes to **1** were made to explore the SAR of this unusual functional group (Table 1). Importantly, replacement of the sulfur with oxygen (**6)** was tolerated, while NH (**7**) was not, and the terminal amino group proved to be very sensitive to change. While a single methyl substituent was tolerated (**3**) a

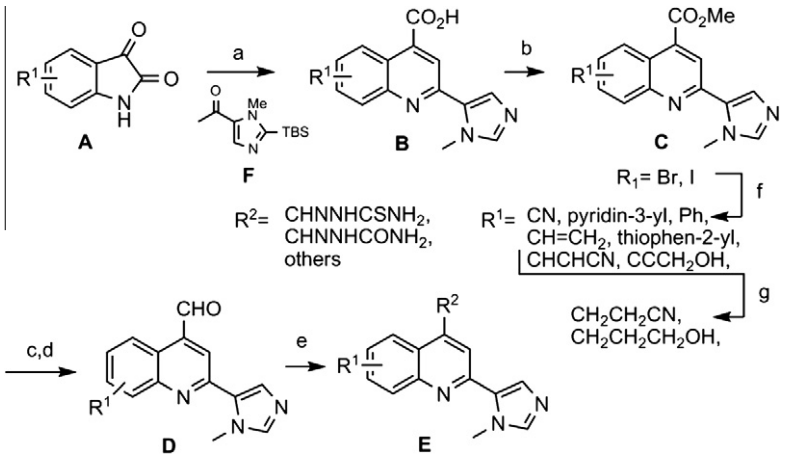

Scheme 1. Reagents and conditions: (a) KOH, EtOH, H_2O 60%; (b) MeOH, H_2SO_4, 80%; (c) Te, $NaBH_4$; (d) Dess–Martin periodinane; (e) AcOH, EtOH, H_2O, semi(thio)carbazide, semicarbazide or nucleophile; (f) $PdCl_2(PPh_3)_2$, CuI, DMF–Et_3N, methyl propargyl ether, or $Pd(PPh_3)_4$, Et_3N, DMF, acrylonitrile; (g) 10%Pd/C, H_2, MeOH.

Table 2
SAR of the quinoline 4-position

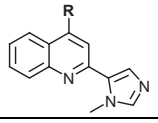	Compound	IKKβ IC_{50} (μM)
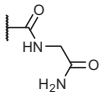	**10**	>30
	**11**	7
	**12**	8.5
	**13**	>30
	**14**	>30
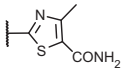	**15**	>30
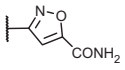	**16**	>30
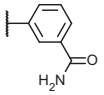	**17**	>30
	**18**	>30
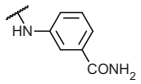	**19**	>30
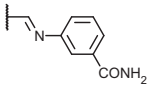	**20**	>30
	**21**	>30
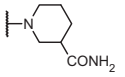	**22**	>30
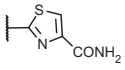	**23**	>30

dimethylamine (**4**) was not tolerated. Interestingly, methylation as in **2** improved potency twofold but an additional methyl group at the terminal NH_2 as **5** was not tolerated. Thus a key element in this SAR was the terminal amine, which proved critical for binding potency.

Additional SAR studies were undertaken to modify this potentially problematic moiety (Table 2). Many analogs (**10**, **15**, **16**, **17**, **22**, and **23**) were made in an attempt to mimic the length and orientation of the semithiocarbazone, but none proved to be very active. Compounds such as **11** and **12**, which retained some of the orientation of the semithiocarbazone moiety, were more potent.

Most efforts to replace or modify the *N*-methyl imidazole moiety were unsuccessful. Five-membered rings such as thiazoles (**25**, **26**), the N-linked imidazole **43**, pyrazole **42**, and the des-methyl analogs **38** and **39** were tolerated when compared to **1** and **6**. The common feature in these analogs was the unhindered 3-aza nitrogen. Compounds with nearly identical architecture but lacking this 3-aza-nitrogen (**24**, **40**, and **41**) were poorly tolerated.

Table 3
SAR of the quinoline 2-position

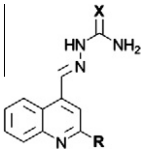

Compds	R	IKKβ IC_{50} (μM)
1		0.25(X = S)
24		>30(X = O)
25		1.2(X = S)
26		1.6(X = O)
27		>30(X = S)
28		>30X = O)
29		>30(X = S)
30		>30(X = S)
31		>30X = O)
32		>30(X = S)
33		>30X = O)
34		>30(X = S)
35		>30(X = S)
36		>30X = O)
37		>30(X = S)
38		7.5(X = S)
39		6.2(X = O)[a]
40		>30(X = S)
41		>30X = O)
42		4.5(X = O)
43		1.75(X = S)
44		>30(X = S)
45		>30(X = S)
46		>30(X = S)
47		>30(X = S)
48		>30X = O)

[a] IC_{50} calculated from measurement at 10 μM.

The potency may be enhanced by the pK_a of the 3-aza-heterocycles. For example, the pK_a of thiazole is 2.52 versus 0.8 for oxazole,[12] the increased potency of **25** and **26** relative to **27** and **28** could be due to the differences in basicity between these analogs. Methyl substituted analogs that sterically hindered the 3-aza nitrogen exhibited a potency decline, indicative of a precise binding orientation or a highly constrained binding pocket. Compare **43** to **29** or **44** and **25** to **46**. The weak potency in **32**, **33**, **35**, and **36**, which all contain 3-aza nitrogen, imply that steric demands take precedence over a putative H-bond contact (Table 3).

Based on the SAR generated around the 2- and 4-quinoline substituent it appeared that both the semithiocarbazone and the *N*-methylimidazole were playing crucial roles in the energetics of enzyme binding. In the absence of enzyme–inhibitor crystallographic

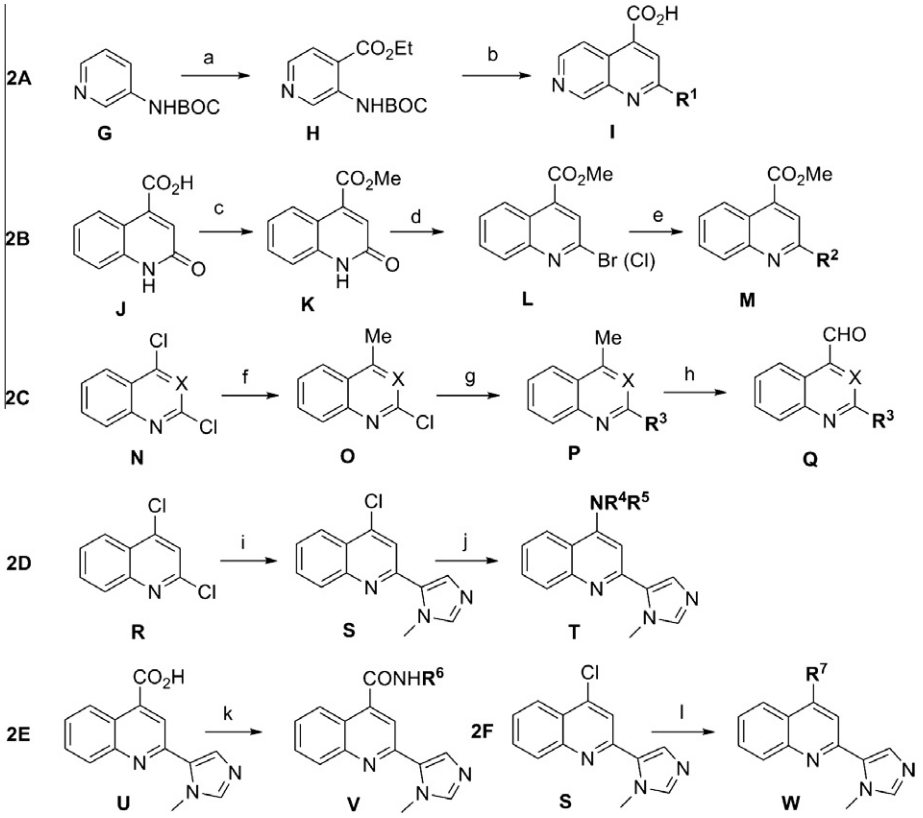

Scheme 2. Reagents and conditions: (a) *n*-BuLi, THF, diethyl oxalate; (b) KOH, $\mathbf{R^1}$-COMe EtOH, H_2O; (c) MeI, K_2CO_3, DMF; (d) $POBr_3$, ($POCl_3$) toluene; (e) $\mathbf{R^2}$-stannane, $Pd_2(dba)_3$, triphenylarsine, CuI, DMF; (f) MeMgCl, $ZnBr_2$, THF; (g) $Pd(PPh_3)_4$, $\mathbf{R^3}$-stannane, CuI, DMF; (h) SeO_2, dioxane; (i) $Pd(PPh_3)_4$, CuI, 1-methy-5-tributylstannylimidazole, DMF 60 °C 3 h; (j) $\mathbf{R^4R^5}NH_2$, 120 °C sealed tube; (k) $SOCl_2$, reflux, then DIPEA DCM, $NH\mathbf{R^6}$; (l) $\mathbf{R^7}$-stannane, $Pd_2(dba)_3$, triphenylarsine, CuI, DMF.

Table 4
SAR around the quinoline core structure

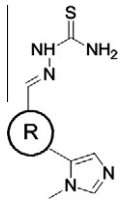

Compds	R	IKKβ IC_{50} (μM)
49		>30
50	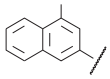	1.8
51	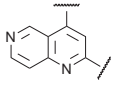	0.42
52	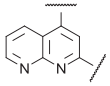	24
53	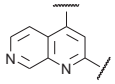	1.2
54	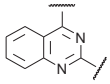	4.6

data we speculate that these moieties were making key contacts to the hinge region of the protein. A model of these inhibitors bound to IKKβ was constructed that had the NH_2 of the semithiocarbazone acting as a H-bond donor to the hinge carbonyl of Gln-100 of IKKβ in the ATP binding domain and the 3-N of the methylimidazole acting as an H-bond acceptor to the –NH of the adjacent Cys-99. All subsequent SAR development was undertaken with this model in mind.

Attempts were made to optimize the core quinoline moiety (Table 4). A pyridine ring (**49**) was not tolerated but a naphthalene core (**50**) had some modest activity. Various other nitrogen containing cores were prepared, with substitutions at the 3-, 6-, 7-, and 8-positions. The 8-aza (**52**) and the 3-aza analog **54** had weak activity. Molecular modeling indicated that the lone pair on the 3-aza analog **54** could have a repulsive interaction with the adjacent nitrogen lone pair of the semithiocarbazone (Fig. 2).

It was intriguing to find that 6-aza (**51**) and 7-aza (**53**) both had a level of potency similar to **1**. This observation led us to explore further substitutions at the 6- and 7-positions. We found that the 6- and 7-methyl analogs, **55** and **57** were more potent than 3-methyl (**56**) and 8-methyl (**58**) (Table 5). Generally, small lipophilic and electron-withdrawing groups (EWG) at the quinoline 7-position were found to improve activity. For example, 7-Me (**57**), 7-CF_3 (**64**), (**65**), 7-Br (**72**), 7-CN (**73**), and 7-Et (**78**) displayed improved IKKβ potency compared to **1** or **6**, and **72** had sub-micromolar cellular activity. However, the activity dropped off with bulkier groups substituted at the 7-position such as *t*-butyl (**66**), *n*-propyl (**74**), and phenyl (**75**).

At the 6-position small groups seemed to have little effect, as can be seen by **55** and **63** compared to **1**, and EWG containing analogs like **62** and **63** were either neutral or detrimental for potency. Additionally, strongly electron donating groups (EDG) like **61** were

Table 5
SAR of the quinoline 6- and 7-positions

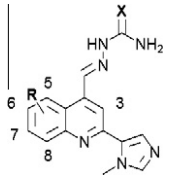

Compds	X	R	IKKβ IC_{50} (μM)	IKKα IC_{50} (μM)	NF-κB IC_{50} (μM)	HWB IC_{50} (μM)
6	O	6,7-H	1.1	25.9	5.9	26
55	S	6-Me	0.23	18.2	—	—
56	O	3-Me	3.0	—	—	—
57	S	7-Me	0.12	1.9	>30	—
58	S	8-Me	>30	—	—	—
59	S	8-Ph	>30	—	—	—
60	O	6-Ph	>30	—	>30	—
61	O	6-OMe	2.95	—	>30	—
62	O	6-CN	3.07	—	>30	—
63	S	6-F	0.26	—	1.0	—
64	S	7-CF_3	0.09	17.2	1.0	—
65	O	7-CF_3	0.7	25.2	1.8	14
66	S	7-*t*-Bu	2.8	>30	>30	—
67	O	7-*t*-Bu	12.6	—	—	—
68	S	6-(Pyridin-3-(yl))	0.32	—	3.0	—
69	S	6-CH_2CH_2CN	0.010	1.6	0.5	2.5
70	O	6-CH_2CH_2CN	0.10	—	10	9.4
71	S	6-$CCCH_2OH$	0.9	>30	30	—
72	S	7-Br	0.06	2.3	0.4	—
73	S	7-CN	0.06	10.6	1	—
74	S	7-Propyl	0.24	0.88	2.5	—
75	S	7-Ph	2.0	20	>30	—
76	S	7-Cyclopropyl	0.13	—	10	—
77	O	7-Cyclopropyl	0.6	—	8	30
78	S	7-Et	0.13	22.5	1.0	—
79	O	7-CH=CH_2	0.6	>30	1.0	31

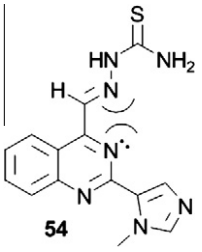

Figure 2. Putative repulsive interactions.

Table 6
Physicochemical and PKDM parameters

Compds	Aq Soln [a] (μg/mL)	Solubility 10% FBS in PBS buffer [b] (μg/mL)	Permeability [c] PAPP (10^{-6} cm/s)	Intrinsic clearance [d] (mL/min/kg)
2	0.26	16.3	71.2	9
6	8.3	>29	15.1	5
65	4.8		10.1	—
79	0.15		13.9	—

[a] pH 6.5.
[b] Turbidity assay.
[c] CaCO-2 cells.
[d] Rat microsomes.

also disfavored. Larger groups were more tolerated, including pyridin-3-yl (**68**) and propynol (**71**), but a real improvement in potency was found with the flexible cyanoethyl containing analogs **69** and **70**. Compound **69** was also potent in cells (0.5 μM in the NF-κB gel-shift assay) although the corresponding semicarbazone (**70**) was 10-fold less active toward IKKβ and had limited cellular activity. In all cases, there was a 4–10-fold biochemical potency difference between the semithiocarbazones and the semicarbazones. For example, semithiocarbazones **64**, **66**, and **76** are more potent than the corresponding semicarbazones **65**, **67**, and **77,** respectively (Table 5).

Table 7
PK parameters

Compds	Rat [a]			Dog [b]	
	Cl (L/h/kg)	V_{diss}(L)	%*F*	Cl (L/h/kg)	%*F*
2	1.9	0.8	54	—	—
6	1.6	1.2	4	1.5 ± 0.8	75 ± 30
65	1.7	0.9	2	—	—
79	1.3	1.1	2	—	—

[a] Males 1 mg/kg iv, 5 mg/kg po.
[b] Female beagles 1 mg/kg iv, 5 mg/kg po.

Because of their poor solubility, we were unable to obtain reliable PK; many of the semithiocarbazones could not be formulated for iv/po administration. However, the semicarbazones proved somewhat more soluble and we were able to measure the exposure in rat and dog. These values were compared with in vitro parameters such as permeability and microsomal clearance (Tables 6 and 7).

Although **2** and **6** had reasonable intrinsic clearance as measured by rat microsomes, the in vivo clearance was considerably higher approaching 50% liver blood flow. In general, the oral exposure was low (2–4%), with a corresponding low CaCo-2 cell permeability (PAPP: 10–15 × 10^{-6} cm/s) for **6**, **65**, and **79**. The

N-methyl semithiocarbazone (**2**) had a PAPP value nearly fivefold higher (71.2×10^{-6} cm/s) with a marked improvement in oral bioavailability (54%). Dog PK was obtained for **6** and found to have an oral bioavailability that was acceptable, but the clearance was 80% liver blood flow, indicating some degree of enterohepatic re-circulation (Table 7).

Initial SAR was developed around the HTS lead **1**. Few changes were tolerated except substitution at the quinoline 6- and 7-positions. There were a few examples of submicromolar activity in cells, notably **69**, which had low micromolar potency in a HWB assay. In general, semithiocarbazones were found to have increased potency relative to the semicarbazones but suffered from poor PK characteristics compared to the semicarbazones. Additional efforts on the further refinement of these analogs are described in part II, which follows this manuscript.

References and notes

1. (a) Solt, L. A.; May, M. J. *Immunol. Res.* **2008**, *42*, 3l; (b) Hacker, H.; Karin, M. *Sci. STKE* **2006**, 357; (c) Woronicz, J. D.; Gao, X.; Cao, Z.; Rothe, M.; Goeddel, D. V. *Science* **1997**, *278*, 866; (d) Regnier, C. H.; Song, H. Y.; Gao, X.; Goeddel, D. V.; Cao, Z.; Rothe, M. *Cell* **1997**, *90*, 373.
2. Bonizzi, G.; Karin, M. *Trends Immunol.* **2004**, *25*, 280.
3. Hu, Y.; Baud, V.; Delhase, M.; Zhang, P.; Deerinck, T.; Ellisman, M.; Jounson, R.; Karin, M. *Science* **1999**, *284*, 316.
4. (a) Karin, M. *Cell Res.* **2008**, *18*, 334; (b) Pande, V.; Ramos, M. J. *Curr. Med. Chem.* **2005**, *12*, 357; (c) Karin, M.; Greten, F. R. *Nat. Rev. Immunol.* **2005**, *5*, 749; (d) Karin, M.; Yamamoto, Y.; Wang, Q. M. *Nat. Rev. Drug Disc.* **2004**, *3*, 17; (e) Luo, J.-L.; Kamata, H.; Karin, M. *J. Clin. Invest.* **2005**, *115*, 2625.
5. Millennium (Takeda) had entered MLN-0415 a small molecule inhibitor of IKKβ in a phase I study in 2006. The structure has not yet been disclosed.
6. (a) Liddle, J.; Bamborough, P.; Barker, M. D.; Campos, S.; Cousins, R. P. C.; Cutler, G. J.; Hobbs, H.; Holmes, D. S.; Ioannou, C.; Mellor, G. W.; Morse, M. A.; Payne, J. J.; Pritchard, J. M.; Smith, K. J.; Tape, D. T.; Whitworth, C.; Williamson, R. A. *Bioorg. Med. Chem. Lett.* **2009**, *19*, 2504; (b) Bouaboula, M.; Tonnerre, B. PCT Int. Appl. WO 2009056693.; (c) Deng, J.; Kerns, J. K.; Jin, Q.; Lin, G.; Lin, X.; Lindenmuth, M.; Neipp, C.; Nie, H.; Thomas, S. M.; Widdowson, K. L. U.S. Patent Appl. Publ. 2009143372.; (d) Fujiwara, H.; Iso, T.; Fujita, K.; Masuda, T.; Higuchi, N.; Hirai, M. PCT Int. Appl. WO 2009075277.; (e) Elder, A. M.; Ghosh, S.; Harrison, S. J.; Hepperle, M. E.; Liu, J. F.; Murray, R. S.; Renou, C. C.; Reynolds, D. PCT Int. Appl. WO 2009067233.; (f) Enomoto, H.; Kawashima, K.; Kudou, K.; Yamamoto, M.; Murai, M.; Inaba, T.; Ishizaka, N. PCT Int. Appl. WO 2008087933.; (g) Moffat, D.; Festus, C.; Davies, S. J.; Charlton, M. H.; Hirst, S. C.; Onions, S. T.; Williams, J. G. PCT Int. Appl. WO 2008053185.; (h) Ginn, J. D.; Sorcek, R. J.; Turner, M. R.; Young, E. R. R. U.S. Patent Appl. Publ. 2007293533.; (i) Hu, Y.; Sum, F.-W.; Di Grandi, M.; Norton, E. U.S. Patent Appl. Publ. 2007244140 2007.; (j) Kim, M. H.; Park, C. H.; Chun, K. W.; Choi, J. W.; Oh, B. K.; Won, R. L.; Jang H.; Kim, K. H.; Kim, S. M. Rep. of Korea 2007040059.; (k) Callahan, J. F; Kerns, J. K.; Lin, X. PCT Int. Appl. WO 2007102883.; (l) Dahnke, K. R.; Lin, H.-S.; Shih, C.; Wang, Q. M.; Zhang, B.; Richett, M. E. PCT Int. Appl. WO 2007092095.; (m) Weber, O.; Ziegelbauer, K.; Seiler, P.; Krahn, T.; Diedrichs, N.; Riedl, B. PCT Int. Appl. WO 200701467.; (n) Beauliu, F.; Ouellett, C.; Ruediger, E. H.; Belema, M.; Qiu, Y.; Yang, X.; Banville, J.; Burke, J. R.; Gregor, K. R.; MacMaster, J. F.; Martel, A.; McIntyre, K. W.; Pattoli, M. A.; Zusi, F. C.; Vyas, D. *Bioorg. Med. Chem. Lett.* **2007**, *17*, 1233; (o) Bingham, A. H.; Davenport, R. J.; Gowers, L.; Knight, R. L.; Lowe, C.; Owen, D. A.; Parry, D. M.; Pitt, W. R. *Bioorg. Med. Chem. Lett.* **2004**, *14*, 409; (p) Murato, T.; Shimada, M.; Sakakibara, S.; Yoshino, T.; Kadono, H.; Masuda, T.; Shimazaki, M.; Shintani, T.; Fuchikami, K.; Sakai, K.; Inbe, H.; Takeshita, K.; Niki, T.; Umeda, M.; Bacon, K. B.; Ziegelbauer, K. B.; Lowinger, T. B. *Bioorg. Med. Chem. Lett.* **2003**, *13*, 913; (q) Castro, A. C.; Dang, L. C.; Soucy, F. G.; Renier, L.; Mazdiyasni, H.; Hottelet, M.; Parent, L.; Pien, C.; Palombella, V.; Adams, J. *Bioorg. Med. Chem. Lett.* **2003**, *13*, 2419.
7. Lawrence, T.; Bebian, M.; Liu, G. Y.; Nizet, V.; Karin, M. *Nature* **2005**, *434*, 1138.
8. (a) Browner, M. F.; Clark, D. L.; Cushing, T. D.; Hao, X.; Hawley, R. C.; He, X.; Jaen, J. C.; Labadie, S. S.; Smith, M.-L.; Talamas, F. X.; Walker, N. P. C.; Labelle, M. U.S. Patent 6846,834 2005.; (b) Browner, M. F.; Clark, D. L.; Cushing, T. D.; Hao, X.; Hawley, R. C.; He, X.; Jaen, J. C.; Labadie, S. S.; Smith, M.-L.; Talamas, F. X.; Walker, N. P. C.; Labelle, M. U.S. Patent 7186,841 2007.; (c) Cushing, T. D.; He, X.; Smith, M.-L.; DeGraffenreid, M. R.; Powers, J.; Tomooka, C.; Clark, D. L.; Hao, X.; Jaen, J. C.; Labelle, M.; Walker, N. P. C.; Gill, A. L.; Talamas, F. X.; Labadie, S. U.S. Patent 7176,314 2007.
9. *The IKKβ biochemical assay was performed in the following manner*: a neutravidin coated 96-well microtiter plate was treated with to 80 μL/well of 1 μM biotinylated IKBα derived substrate peptide (KKERLLDDRHDSGLDSMKDEEYE-QGK-bio) and buffer (20 mM Tris–HCl, pH 7.5, 10 mM $MgCl_2$, 2 mM EGTA, 1 mM NaF, 0.5 mM benzamide, 1 mM DTT, 0.1% NP-40, 10% μM ATP). Compound was added (10 μL/well) in DMSO from 1 nM to 30 μM followed by 10 mL buffer and baculovirus produced (insect cells) full-length recombinant IKKβ. The mixture was incubated at rt for 45 min, after which the reaction was stopped by washing the plates 3× with 150 μL H_2O. At this time, 2% BSA in PBS 100 μL/well and primary monoclonal antibody recognizing the phosphorylated epitope at 1:10,000 dilution, premixed with conjugated anti-mouse secondary antibody horse-radish peroxidase (HRP) 1:10,000 dilution. The solution was incubated on a shaker at rt for 40 min then washed 3× 150 μL H_2O. SuperSignal HRP (Pierce), 100 mL/well 10× diluted was added and incubated 5 min. The chemiluminescent signal was found with a Labsystems LuminoSkan luminometer. IC_{50}s were determined by curve fitting with LSW data analysis software (MDL).
10. NF-kB gel shift assays were carried out as described (Schindler, U.; Baichwal, V. R. *Mol. Cell Biol.* **1994**, *14*, 5820). In summary, IL8/ECV304 cells were stimulated with TNF for 1 h in the absence or presence of compounds and NF-kB. DNA binding activity was determined by gel shift experiments from crude nuclear extracts.
11. *Human whole blood assay*: blood samples in a 96-well microtiter plate were stimulated for 5 h with LPS in the presence or absence of test compounds. Following the incubation period, levels of TNF in the culture supernatants were determined with an ELISA kit (R&D systems).
12. Zoltewicz, J. A.; Deady, L. W. *Adv. Heterocycl. Chem.* **1978**, *22*, 71.